THRESHOLD SENSITIVITY AND OUTLET VERIFICATION IN DEM-DERIVED DRAINAGE EXTRACTION: A DIGITAL MAPPING FROM KHOBRAGADI RIVER CATCHMENT OF PENINSULAR INDIA

Gunwant G. Wadpalliwar[1*], *Imran Sheikh* [2] , Sadhana S. Kambale[3] Shrutika R. Kamble[4*], Harshita V. Wadikar[5],

[1*] *Shri. Govindrao Munghate Arts and Science College Kurkheda District Gadchiroli.*

[2] *District Mining Officer,Collectorate Gadchirol, Maharashtra.*

[3] *Shri. Govindrao Munghate Arts and Science College Kurkheda District Gadchiroli.*

[4] *Shri. Govindrao Munghate Arts and Science College Kurkheda District Gadchiroli.*

[5] *Shri. Govindrao Munghate Arts and Science College Kurkheda District Gadchiroli.*

Corresponding Author: [1*] *Gunwant G. Wadpalliwar ggwadpalliwar@gmail.com*

Abstract

A multiscale geospatial assessment was undertaken for the Bandia, Khobragadi, Kathani, Sati and Gadhavi river systems in Gondia and Gadchiroli districts, eastern Maharashtra. Regional drainage context was established from HydroBASINS, MERIT Hydro, OpenStreetMap and a drainage network derived from 30 m NASADEM data. Flow-accumulation thresholds of 1,000, 2,500, 5,000 and 10,000 cells were tested, and a 5,000-cell threshold was retained as a study-specific analytical compromise. The Khobragadi watershed was validated as the quantitative pilot and was characterized by an area of 1,833.608 km², a perimeter of 408.676 km, 749.814 km of extracted streams and a drainage density of 0.409 km km⁻². Fifth-order organization was reached, and 49.0% of mapped stream length was represented by first-order segments. Long-term JRC data indicated that 95.6% of historically detected water was non-permanent or seasonal. For 2025, a 4.66-fold post-monsoon expansion in Sentinel-2-derived surface-water extent was identified. Strong outlet sensitivity was demonstrated by the rejected Sati delineations. Regional mapping was therefore found to support river-system characterization, whereas locally verified outlets were required before basin-specific morphometry could be reported.

Keywords: *Watershed delineation; Drainage morphometry; NASADEM; Surface-water dynamics; Monsoon hydrology.*

I. INTRODUCTION

Watersheds are functional landscape units within which terrain, drainage, land cover, soils, geology, rainfall and human water use are interconnected. The partitioning of precipitation among runoff, temporary storage, infiltration and downstream flow is governed by their configuration. In monsoon-influenced agricultural regions, pronounced differences between wet- and dry-season water availability may occur even where annual rainfall is substantial. Consequently, reliable basin boundaries, a hydrologically meaningful drainage network, quantitative morphometry and seasonal surface-water information are required in addition to a simple inventory of mapped rivers.

A practical framework for integrating these forms of evidence is provided by remote sensing and geographic information systems (GIS). Drainage extraction and watershed delineation can be supported by digital elevation models (DEMs), while repeated observations of surface water can be obtained from satellite imagery. The value of integrated geoinformatics for water-resource monitoring, modelling and decision support has been emphasized in recent research (Jagadeesha & Manavalan, 2025). Within India, geospatial methods have also been applied to agricultural water management, land and water conservation and environmental monitoring (Singh et al., 2023; Tarate et al., 2024).

The reliability of basin-scale assessment is nevertheless controlled by the quality and spatial scale of the hydrographic representation. More consistent depictions of drainage pathways and drainage-density variability have been provided by global products such as Hydrography90m and MERIT-derived river networks (Amatulli et al., 2022; Lin et al., 2021). It has also been demonstrated through multi-source fusion and deep-learning studies that every headwater, seasonal channel or locally modified watercourse cannot be represented by a single dataset (Liu et al., 2026; Pierson & Mehrabi, 2024). Regional products are therefore valuable for hydrographic orientation, but local stream alignment, confluences, outlets and basin boundaries must be verified before basin-specific measurements are derived.

This requirement is especially relevant in Gondia and Gadchiroli districts of eastern Maharashtra, where the Wainganga-Pranhita-Godavari drainage setting, extensive rural land use, forested terrain and monsoonal seasonality produce a complex water-resource context. Five named river systems-Bandia, Khobragadi, Kathani, Sati and Gadhavi-were considered. Regional characterization was undertaken for all five systems, whereas detailed basin-scale assessment was restricted to a hydrologically validated pilot watershed.

Previous research in Maharashtra and elsewhere in India has shown that DEM-derived morphometry and remotely sensed water observations can support watershed characterization (Pande et al., 2021; Singh et al., 2023). However, automated basin boundaries are sometimes accepted without adequate verification of the outlet or main-stem confluence, and seasonal surface-water evidence is often interpreted without sufficient attention to classification sensitivity. These limitations were addressed through multi-source drainage comparison, pilot-based outlet validation, explicit rejection of implausible delineations and threshold testing of both drainage extraction and surface-water classification.

Accordingly, a reproducible multiscale geospatial workflow was developed to characterize regional drainage, evaluate drainage-network thresholds, validate a pilot watershed and assess seasonal surface-water dynamics. The following objectives were addressed:

- to evaluate alternative flow-accumulation thresholds and select a suitable network for outlet verification and watershed delineation;
- to delineate and validate the Khobragadi pilot watershed and quantify its principal drainage and morphometric characteristics;
- to assess long-term and 2025 seasonal surface-water characteristics within the validated Khobragadi watershed using JRC and Sentinel-2 data; and
- to evaluate drainage alignment, outlet-placement sensitivity and surface-water classification sensitivity, including the exploratory Sati outlet experiment.

A transparent distinction was maintained between regional drainage evidence and validated basin-specific results. The workflow was intended to guide subsequent field verification and detailed hydrological investigation rather than replace discharge monitoring, hydrogeological testing or engineering assessment.

2. LITERATURE REVIEW

2.1 Hydrographic data and drainage-network representation

River-network representation is not a neutral cartographic choice. Calculated stream order, channel length and drainage density are affected by headwater inclusion, topology, channel-extraction rules and the treatment of flat or internally drained terrain. A globally consistent hydrographic network at approximately 90 m resolution was provided by Hydrography90m, with improved representation of smaller streams relative to many earlier products (Amatulli et al., 2022). Spatial variability in drainage density was also incorporated into a MERIT-derived global vector network by Lin et al. (2021).

A shift from reliance on individual datasets toward multi-source integration has been observed. Complementary river datasets were fused by Liu et al. (2026) to improve spatial accuracy and topology, while global waterways were mapped from Sentinel-2 imagery and a DEM by Pierson and Mehrabi (2024). Drainage extraction should therefore be treated as a validation problem in which the strengths and limitations of independent sources are compared, particularly where small or seasonal channels are important. Morphometric Analysis of Gadhvi River, Sub-Basin Using Remote Sensing and GIS techniques. Application of morphometric Study For Groundwater Management In Dongargarh Granite Around Kurkheda, District Gadchiroli, Maharashtra. Gunwant G. W. et al (2024)

Regional drainage systems can be placed within nested hydrographic contexts through products such as HydroSHEDS and related datasets (Hou et al., 2025). Their principal advantage is large-area consistency, whereas their principal limitation for local delineation is spatial scale. A hierarchical workflow is consequently required: regional products can be used to establish the broader Wainganga and Indravati setting, but locally processed elevation data and verified outlets should be used to define basin boundaries and stream metrics.

2.2 OpenStreetMap as a hydrographic reference

Named waterways and approximate river alignments can be obtained from OpenStreetMap (OSM), which is particularly useful for locating confluences and retaining local river identity. In this study, the Western Zone India extract supplied by Geofabrik GmbH (2026) was used as an independent reference rather than as the sole hydrological network. Such separation is necessary because the completeness of volunteered geographic information varies spatially and temporally, and local checks are required before analytical use (Monteiro & Patrício, 2024).

Complementary error structures are associated with OSM and DEM-derived streams. An OSM line may be laterally displaced, generalized, unnamed or absent, whereas a DEM-derived channel may be affected by elevation resolution, artificial depressions, flat terrain or infrastructure. Confidence is increased where agreement is observed, but disagreement cannot be resolved by assuming that either source is automatically correct. Accordingly, OSM alignments were compared with flow accumulation, terrain continuity and satellite imagery during outlet verification.

2.3 Watershed morphometry and drainage interpretation

Basin geometry and drainage organization are translated into quantitative descriptors through morphometric analysis. Network structure is represented by linear parameters such as stream order, stream count and stream length, while basin dissection and form are represented by areal parameters such as drainage density. The reliability of these measures is dependent on DEM quality, extraction threshold, network topology and consistent measurement rules. Methodological risks associated with variable input quality and incomplete testing of Horton-type relationships have been emphasized by Shekar and Mathew (2024).

The use of remote sensing, GIS and morphometric assessment for watershed characterization in Maharashtra has been demonstrated by Pande et al. (2021), while the role of morphometric evidence in land- and water-conservation prioritization has been reviewed by Singh et al. (2023). Nevertheless, morphometric indices do not constitute a complete hydrological model. Drainage density and stream-order patterns must be interpreted with reference to terrain, lithology, vegetation, rainfall, source resolution and extraction threshold.

In the present study, topology-dependent Horton stream numbers and bifurcation ratios were not inferred from raw vector segments. Instead, the validated Khobragadi pilot was characterized using basin area, perimeter, total extracted stream length, drainage density, maximum Strahler order and order-wise segment lengths. This restricted parameter set was adopted to prevent raster-to-vector segmentation artefacts from being interpreted as conventional branching statistics.

2.4 Remote sensing of seasonal surface water

Seasonal surface-water mapping is affected by sensor resolution, cloud and shadow, vegetation, turbidity, wet soil and the classification rule applied. Multi-temporal analysis is therefore more informative than a single-date classification because permanent water, seasonal expansion and dry-season persistence have different hydrological meanings. The importance of sensor selection, temporal sampling and accuracy assessment in water-related mapping has been demonstrated in the broader remote-sensing literature (Yuan et al., 2025).

For agricultural water management in India, remote sensing and GIS have been identified as cost-effective approaches for monitoring hydrological conditions over extensive areas (Tarate et al., 2024). In the present analysis, long-term JRC surface-water classes were combined with Sentinel-2 pre- and post-monsoon composites. Because the products represent different periods, spatial resolutions and class definitions, direct equivalence between their mapped areas was not assumed.

Mapped surface-water area was treated as evidence of occurrence, persistence and seasonal expansion rather than as a measurement of groundwater recharge, discharge or storage volume. This distinction is essential because surface-water area does not provide water depth, hydraulic connectivity or subsurface information.

2.5 Research gap and analytical scope

Global hydrography, OSM river mapping, DEM-derived drainage extraction and seasonal surface-water classification are frequently applied as separate analytical components. Fewer regional studies have linked these components through an explicitly documented outlet-validation procedure in which implausible watershed outputs are rejected rather than reported as final boundaries.

The present study was designed to address this gap through a multiscale evidence hierarchy. Regional hydrographic datasets were used to characterize five named river systems, while detailed morphometry and surface-water analysis were restricted to the validated Khobragadi pilot. The Sati case was retained as methodological evidence of outlet sensitivity, and the remaining river systems were reported only at the regional-reference level.

This design allowed uncertainty to be carried into interpretation. Quantitative comparisons were not extended to river systems for which outlets and basin boundaries had not been validated, and surface-water changes were interpreted as mapped areal changes rather than as direct hydrological fluxes.

3. METHODOLOGY

3.1 Research design and analytical environment

A sequential multiscale geospatial design was applied. Regional hydrographic products were first used to establish the broader drainage context. A conditioned DEM was then used to derive drainage pathways and evaluate flow-accumulation thresholds. Outlet verification and watershed delineation were undertaken for the Khobragadi pilot, while the Sati system was used to test outlet sensitivity. Morphometric and surface-water analyses were subsequently restricted to the validated Khobragadi watershed.

Google Earth Engine (GEE) was used for the preparation of raster and time-series datasets (Gorelick et al., 2017). Coordinate-system management, vector editing, cartography, spatial statistics and final integration were undertaken in

QGIS 4.2.0 (Belém do Pará). WhiteboxTools, accessed through the QGIS processing environment, was used for DEM conditioning, D8 flow analysis, pour-point snapping, watershed delineation and stream-network operations (Lindsay, 2016). The D8 procedure was based on the deterministic eight-neighbour flow-routing method developed by O'Callaghan and Mark (1984). Measurement-based processing was undertaken in WGS 84/UTM Zone 44N (EPSG:32644), while geographic layers required by GEE were maintained in WGS 84 (EPSG:4326).

3.2 Study area and analytical units

Gondia and Gadchiroli districts in eastern Maharashtra, India, constituted the study area. The two district polygons were selected from the administrative boundary dataset, repaired and retained as separate features within a combined study-area layer. Geographic versions were prepared in EPSG:4326 for GEE processing, whereas projected measurements were undertaken in EPSG:32644.

Five named river systems were considered: Bandia, Khobragadi, Kathani, Sati and Gadhavi. Regional drainage context was characterized for all five systems. Khobragadi was processed as the validated pilot watershed, Sati was examined as an exploratory outlet-sensitivity case, and Bandia, Kathani and Gadhavi were retained at the regional-reference level. Basin identity was defined by hydrological contribution to a verified outlet rather than by administrative boundaries or the mapped extent of an OpenStreetMap river line (Geofabrik GmbH, 2026).

3.3 Data sources and preparation

The geospatial datasets and their analytical roles are summarized in Table 1. Each dataset was projected or transformed as required, clipped to the appropriate study extent and checked for geometric or raster inconsistencies before analysis.

Table 1. Geospatial datasets used in the analysis and their analytical roles.

Dataset or source	Role in the study	Preparation and use
District administrative boundaries	Study-area definition and clipping	District polygons were repaired; geographic and projected versions were prepared in EPSG:4326 and EPSG:32644, respectively.
HydroBASINS (Lehner & Grill, 2013) and MERIT Hydro (Yamazaki et al., 2019)	Regional basin context and drainage comparison	The products were used to establish the broader Wainganga–Indravati drainage setting and to compare regional drainage alignment.
NASADEM, 30 m (NASA Jet Propulsion Laboratory, 2020)	Terrain, flow direction, accumulation, drainage and watershed delineation	The DEM was clipped, reprojected to EPSG:32644 and hydrologically conditioned before D8 processing.
Geofabrik OSM Western Zone extract (Geofabrik GmbH, 2026)	Named-river reference and confluence identification	River features were projected and compared with DEM-derived drainage; OSM was not used as the sole hydrological network.
Sentinel-2 imagery, 2025 (Drusch et al., 2012)	Pre- and post-monsoon surface-water mapping and visual interpretation	Seasonal composites were prepared, MNDWI was calculated following Xu (2006), and thresholds of 0.00, 0.10 and 0.20 were evaluated.
JRC Global Surface Water (Pekel et al., 2016)	Long-term permanent and non-permanent/seasonal water reference	Historical surface-water classes ending in 2021 were summarized at 30 m resolution within the validated watershed.
High-resolution satellite imagery	Contextual checking of channels, outlets and mapped water	Imagery was used for visual corroboration only and was not treated as a hydrological network.

The broader basin hierarchy was represented using HydroBASINS (Lehner & Grill, 2013), while MERIT Hydro was used as an additional reference for regional drainage alignment and upstream connectivity (Yamazaki et al., 2019).

3.4 DEM conditioning and drainage extraction

A 30 m NASADEM was used as the elevation input for drainage extraction and watershed delineation (NASA Jet Propulsion Laboratory, 2020). The DEM was clipped to an extent that included the upstream contributing areas of the candidate outlets and was reprojected to EPSG:32644. NoData margins and anomalous values were checked, and depression breaching was applied through WhiteboxTools to establish hydrologically connected downslope pathways (Lindsay, 2016). A D8 flow-direction pointer and a flow-accumulation raster were generated from the conditioned DEM following the deterministic eight-neighbour routing approach of O'Callaghan and Mark (1984).

Candidate stream rasters were produced at flow-accumulation thresholds of 1,000, 2,500, 5,000 and 10,000 contributing cells. At 30 m resolution, these thresholds represented nominal contributing areas of approximately 0.90, 2.25, 4.50 and 9.00 km^2, respectively. The derived networks were compared with terrain convergence and reference river alignments. A threshold of 5,000 cells was retained as the study-specific compromise because major and intermediate drainage pathways were preserved while excessive short segments were reduced.

The selected raster network was classified using the Strahler stream-ordering method (Strahler, 1957) and was subsequently converted to vector linework. Stream-order attributes were retained during clipping and length calculation. Raw vector-segment counts were reported separately from topology-corrected Horton stream numbers because segmentation can be introduced during raster-to-vector conversion.

3.5 Outlet verification and watershed delineation

Each named reference river was traced toward its downstream confluence using the Geofabrik OpenStreetMap river extract (Geofabrik GmbH, 2026). A provisional outlet was placed on the corresponding DEM-derived tributary immediately upstream of the receiving channel so that capture of the larger main-stem basin could be avoided. Snapping was restricted to the extracted drainage network.

Candidate outlets were snapped to valid drainage cells using the Whitebox Jenson snap-pour-point procedure (Lindsay, 2016). An initial search radius of 30 m was applied, and a radius of up to 60 m was used only where minor positional disagreement had been confirmed visually. Snapped points were stored in EPSG:32644 and supplied to the Whitebox Watershed algorithm with the non-ESRI D8 pointer.

Each delineation was evaluated against the ordered drainage network, the named reference river, the expected downstream connection and the regional drainage setting. Outputs were rejected where an evident upstream tributary was omitted, the receiving main stem was captured, a drainage divide was crossed implausibly or an incorrectly positioned outlet was indicated. The accepted Khobragadi raster was polygonized, filtered to the basin class, converted to GeoPackage and checked for valid geometry. Repeated Sati outputs were rejected because implausibly small contributing areas were produced.

3.6 Morphometric analysis

The selected stream network was clipped to the validated Khobragadi boundary. Segment length was calculated in kilometres and summarized by Strahler order. Basin area, perimeter, total extracted stream length, drainage density, maximum Strahler order and raw vector-segment count were calculated as defined in Table 2. All distance- and area-based measurements were derived in EPSG:32644.

Table 2. Morphometric quantities calculated for the validated Khobragadi pilot watershed.

Quantity	Calculation or definition	Reporting role
Basin area (A)	Area of the validated watershed polygon	Total contributing area in km²
Basin perimeter (P)	Length of the validated watershed boundary	Boundary length in km
Total extracted stream length	Sum of mapped stream-segment lengths	Total channel length in km
Drainage density (Dd)	Total extracted stream length / A	Mapped channel length per unit area (km km^{-2})
Maximum Strahler order	Highest order represented in the clipped network	Maximum network organization under the adopted threshold
Raw vector-segment count	Count of vector line features after extraction and conversion	Reported separately from topology-corrected Horton stream number

Drainage density was calculated as total extracted stream length divided by basin area. Because the mapped network was dependent on the 30 m DEM and the selected 5,000-cell threshold, the resulting value was interpreted as the density of the adopted extracted network rather than as a threshold-independent basin property.

3.7 Surface-water mapping and seasonal comparison

Long-term surface-water occurrence was characterized using the 30 m JRC Global Surface Water dataset, which represents historical observations from 1984 to 2021 (Pekel et al., 2016). Within the validated Khobragadi watershed, JRC classes were grouped into permanent water and non-permanent or seasonal water. Pixels outside these classes were described as not detected as surface water by JRC at 30 m resolution rather than as locations containing no water.

Seasonal surface-water conditions in 2025 were evaluated using Sentinel-2 multispectral imagery (Drusch et al., 2012). A pre-monsoon composite was prepared for March–May 2025, and a post-monsoon composite was prepared for October–December 2025. Cloud-affected observations were screened before the seasonal composites were generated.

Surface water was classified using the Modified Normalized Difference Water Index proposed by Xu (2006). The index was calculated from the Sentinel-2 green band (B3) and short-wave infrared band (B11) as:

$$\mathrm{MNDWI} = \frac{\mathrm{Green} - \mathrm{SWIR1}}{\mathrm{Green} + \mathrm{SWIR1}}$$

An MNDWI threshold of 0.10 was adopted for the principal classification. Thresholds of 0.00 and 0.20 were also applied to evaluate the sensitivity of the mapped surface-water extent to the selected classification rule. The resulting pre- and post-monsoon water masks were compared spatially to distinguish persistent water, pre-monsoon-only water and post-monsoon-only water.

A five-pixel minimum-mapping filter was applied to the adopted post-monsoon classification to remove isolated very small patches. The retained water polygons were grouped into three size classes: small (<1 ha), medium (1–10 ha) and large (≥10 ha). Classification patterns were visually checked against the corresponding true-colour Sentinel-2 composites. Potential uncertainty associated with mixed pixels, terrain shadows, wet soil, vegetation, turbidity and narrow channels was considered during interpretation.

3.8 Validation, sensitivity and reproducibility

Drainage validation was based on agreement among terrain convergence, flow accumulation and independent river references. Outlet validation required placement on the intended tributary, an appropriate accumulation value and correct downstream connectivity. Surface-water robustness was evaluated by repeating the classification at three MNDWI thresholds and comparing the direction and magnitude of seasonal change.

Uncertainty was attributed to DEM resolution and conditioning, positional disagreement in reference river lines, satellite resolution, seasonal compositing and classification threshold. Processing parameters, coordinate systems, layer versions and intermediate outputs were retained in the project archive to support reproducibility.

4. RESULTS

4.1 Regional drainage framework of Gondia and Gadchiroli

Bandia, Khobragadi, Kathani, Sati and Gadhavi were identified as the five named river systems considered in the regional assessment. Their approximate alignments and downstream relationships were situated within the broader Wainganga-Indravati drainage environment by comparison of HydroBASINS, MERIT Hydro, OSM and DEM-derived drainage evidence.

Broad agreement was observed in the position and orientation of the principal drainage corridors, but exact spatial correspondence was not obtained throughout the study area. Local lateral displacement, differences in line generalization and variable representation of smaller tributaries were identified. The strongest differences occurred where mapped river lines did not coincide with cells of high flow accumulation in the DEM-derived network.

The regional products were most useful for identification of broad drainage relationships, whereas the DEM-derived network was used to represent continuous terrain-controlled connectivity. Consequently, reference river lines were treated as hydrographic and locational evidence rather than as complete representations of the connected drainage network.

Regional agreement was not considered sufficient for acceptance of an individual watershed boundary. Khobragadi was retained as the validated quantitative pilot, Sati was retained as an exploratory outlet-sensitivity case, and Bandia, Kathani and Gadhavi were retained at the regional-context level. The resulting evidence hierarchy is summarized in Table 3.

Quantitative basin metrics were therefore restricted to Khobragadi. Basin areas, drainage densities and other basin-specific morphometric values were not reported for Sati, Bandia, Kathani or Gadhavi because validated boundaries were unavailable.

Table 3. Analysis and evidence levels of the five regional river systems.

River system	Analysis level	Evidence reported
Khobragadi	Detailed validated pilot	Validated watershed boundary, morphometry, stream order and surface-water characteristics
Sati (Satti)	Exploratory	Reference-river identification, outlet sensitivity and rejected provisional delineations
Bandia	Regional context	Named reference river and regional drainage mapping
Kathani	Regional context	Named reference river and regional drainage mapping
Gadhavi	Regional context	Named reference river and regional drainage mapping

4.2 DEM processing and drainage-network selection

Regional drainage extraction was undertaken from the 30 m NASADEM in EPSG:32644. Following depression breaching and hydrological conditioning, D8 flow direction and flow accumulation were derived. Networks were then extracted at thresholds of 1,000, 2,500, 5,000 and 10,000 contributing cells.

The density of mapped drainage was progressively reduced as the contributing-cell threshold was increased. Numerous short headwater and minor channel segments were generated at 1,000 cells, while a comparatively dense lower-order network was retained at 2,500 cells. At 10,000 cells, the network was dominated by principal channels and larger tributaries, and several intermediate drainage pathways were omitted.

The most suitable balance for the regional analysis was provided by the 5,000-cell threshold. Major river courses and intermediate tributaries were retained, whereas the excessive short-channel representation observed at lower thresholds was reduced. Overall correspondence with the principal reference-river corridors was also improved, although local alignment differences remained.

The 5,000-cell network was therefore adopted for outlet verification, watershed delineation and stream-order analysis. Regional Strahler ordering reached sixth order within the full analysis extent.

The selected threshold was treated as a study-specific analytical compromise rather than as a universally optimal value. Total stream length, drainage density, headwater representation and maximum stream order remained sensitive to both the DEM resolution and the extraction threshold.

4.3 Validated Khobragadi pilot watershed

A spatially coherent upstream watershed was produced by the verified Khobragadi outlet. The accepted boundary followed the expected drainage divides and enclosed the tributary network draining toward the selected outlet. An area of 1,833.608 km² and a perimeter of 408.676 km were obtained.

After the selected 5,000-cell network had been clipped to the validated boundary, 749.814 km of mapped streams were retained. A drainage density of 0.409 km km^{-2} was consequently obtained. This value represents the density of the network extracted under the adopted DEM resolution and threshold.

A maximum Strahler order of five was reached. A total of 241 raw vector segments was produced by extraction, conversion and segmentation. This value was treated as a raw vector-segment count and not as a topology-corrected Horton stream number.

The principal morphometric results are summarized in Table 4.

Table 4. Morphometric summary of the validated Khobragadi pilot watershed.

Parameter	Result
Basin area	1,833.608 km²
Basin perimeter	408.676 km
Total extracted stream length	749.814 km
Drainage density	0.409 km km⁻²
Maximum Strahler order	5
Raw vector-segment count	241

4.4 Khobragadi stream-order characteristics

Five Strahler orders were represented within the validated Khobragadi network. The 241 raw vector segments had a combined mapped length of 749.814 km, and their order-wise distribution is summarized in Table 5.

First-order channels were dominant, with 121 segments and a combined length of 367.203 km. Thus, 49.0% of the total mapped stream length was represented by first-order segments. Second-order channels contributed a further 171.426 km, equivalent to 22.9% of total length.

A general decrease in total stream length was observed toward higher orders. Third- and fourth-order channels contributed 102.236 km (13.6%) and 92.439 km (12.3%), respectively, while fifth-order channels represented only 16.510 km (2.2%).

The raw segment count declined from first to third order but increased from 30 third-order segments to 34 fourth-order segments. This irregularity was attributed potentially to raster-to-vector segmentation, tributary splitting or multipart topology and was not interpreted as a conventional Horton bifurcation pattern.

Because topology-corrected stream numbers were unavailable, bifurcation ratios and a mean bifurcation ratio were not calculated from the raw vector-segment counts.

Table 5. Stream-order characteristics of the DEM-derived drainage network within the validated Khobragadi watershed.

Strahler order	Raw vector segments	Total length (km)	Share of total length
1	121	367.203	49.0%
2	48	171.426	22.9%
3	30	102.236	13.6%
4	34	92.439	12.3%
5	8	16.510	2.2%
Total	241	749.814	100%

4.5 Long-term surface-water characteristics

A total of 12.860 km² of historically detected surface water was identified within the validated Khobragadi watershed from the JRC product, equivalent to 0.701% of the basin area. The spatial distribution is shown in Figure 1, and the class statistics are summarized in Table 6.

Non-permanent or seasonal water was dominant and covered 12.291 km², equivalent to 0.670% of the basin area and 95.6% of historically detected water. Permanent water covered 0.569 km², equivalent to 0.031% of the basin and 4.4% of detected water.

The non-permanent or seasonal area was approximately 21.6 times the permanent-water area. Strong seasonal dependence in mapped water occurrence was therefore indicated, but water-storage capacity, discharge and groundwater recharge were not measured by these classes.

Locations outside the mapped classes were interpreted as not detected as surface water by JRC at 30 m. Narrow channels, small ponds, water beneath vegetation and brief inundation may not have been represented consistently

Table 6. Long-term JRC surface-water characteristics within the validated Khobragadi watershed.

JRC surface-water class	Area (km²)	Basin area (%)	Share of historically detected water
Non-permanent/seasonal water	12.291	0.670	95.6%
Permanent water	0.569	0.031	4.4%
Total historically detected water	12.860	0.701	100%

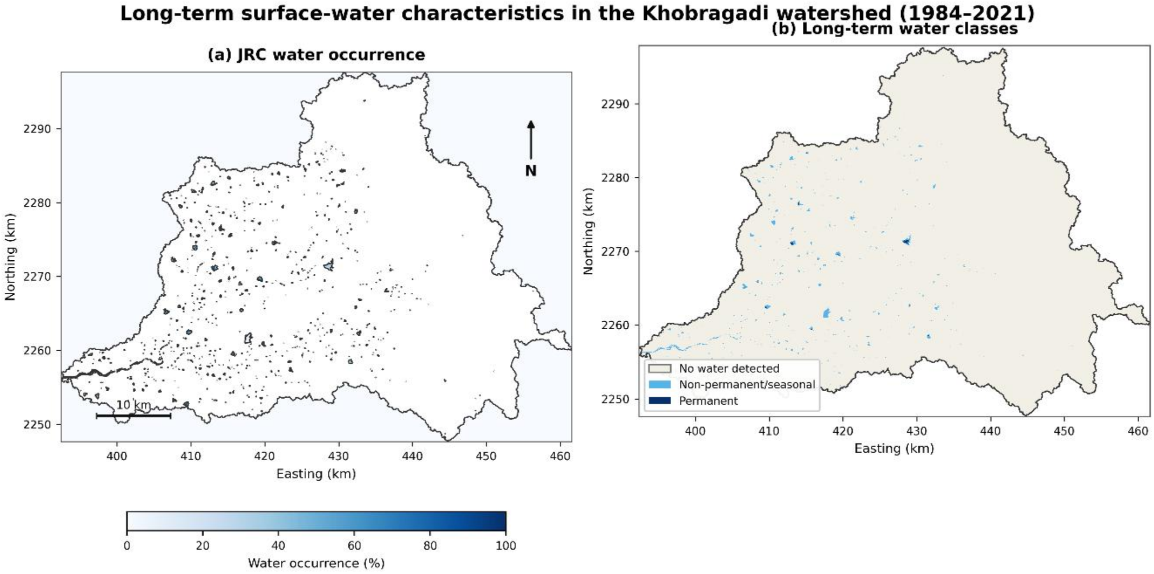

Figure 1. Long-term JRC surface-water characteristics within the validated Khobragadi watershed, showing permanent and non-permanent or seasonal water classes.

4.6 Pre- and post-monsoon surface-water dynamics in 2025

A substantial post-monsoon increase in mapped surface-water extent was identified in 2025. Pre-monsoon water covered 2.802 km² (0.153% of the basin), whereas post-monsoon water covered 13.053 km² (0.712%). The seasonal classes are shown in Figure 2, and the corresponding statistics are summarized in Table 7.

A net increase of 10.250 km² was obtained, corresponding to 0.559 percentage points of basin area. Post-monsoon surface-water extent was 4.66 times the pre-monsoon extent.

Of the mapped pre-monsoon water, 2.757 km² persisted after the monsoon. This persistent component represented 98.4% of the pre-monsoon extent, while only 0.045 km² was classified as pre-monsoon-only water.

Post-monsoon-only water covered 10.295 km² and represented 78.9% of the total mapped post-monsoon extent. Seasonal expansion therefore accounted for most of the post-monsoon water distribution.

The mapped increase represents a change in classified surface area and should not be interpreted as groundwater recharge, storage volume or discharge. The visual contrast between the two seasonal Sentinel-2 composites is presented in Figure 3.

Table 7. Pre- and post-monsoon surface-water statistics for the Khobragadi watershed in 2025.

Indicator	Area (km²)	Basin area (%)
Pre-monsoon water	2.802	0.153
Post-monsoon water	13.053	0.712
Persistent water	2.757	0.150
Pre-monsoon-only water	0.045	0.002
Post-monsoon-only water	10.295	0.561
Net seasonal increase	10.250	0.559 percentage points

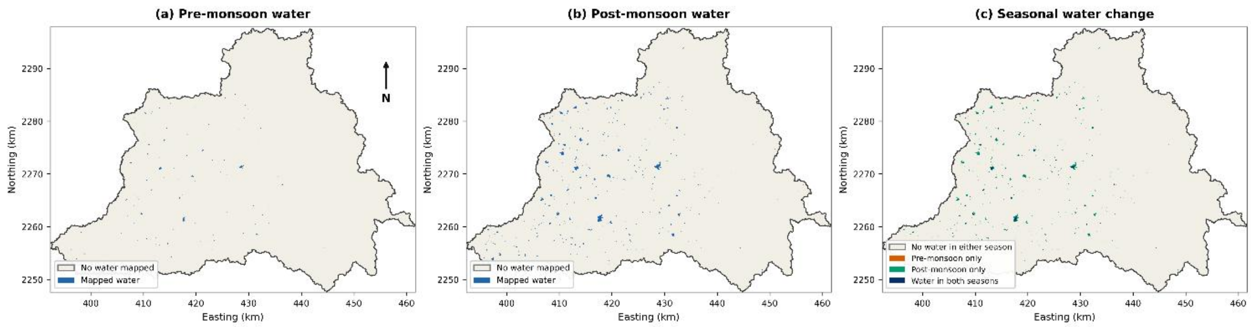

Figure 2. Pre-monsoon, post-monsoon and seasonal-change distribution of mapped surface water within the Khobragadi watershed in 2025.

The pre-monsoon composite showed comparatively dry surface conditions and limited visible open water, whereas darker vegetation and more extensive water features were visible in the post-monsoon composite (Figure 3).

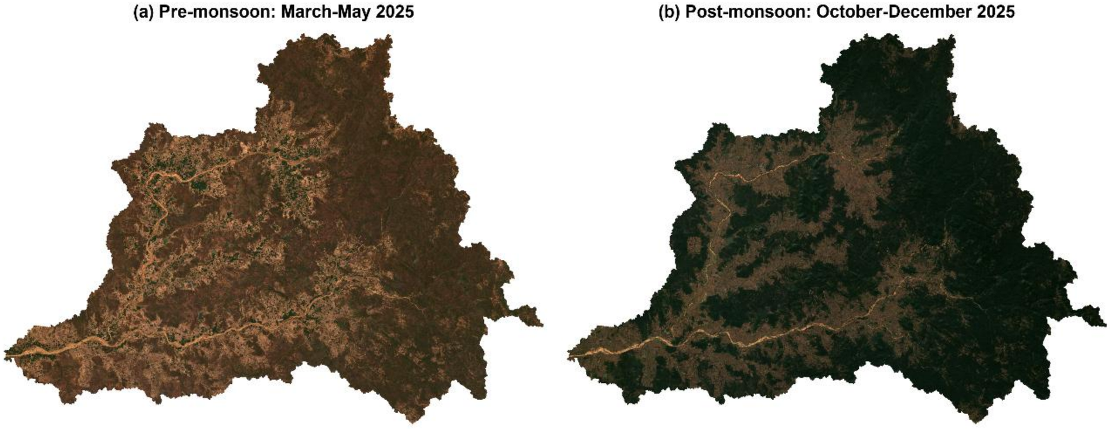

Figure 3. Pre- and post-monsoon true-colour Sentinel-2 composites of the Khobragadi watershed in 2025.

4.7 CLASSIFICATION ROBUSTNESS AND WATER-BODY INVENTORY

4.7.1 MNDWI-threshold sensitivity

The magnitude of mapped surface-water extent varied with the MNDWI threshold, but the direction of seasonal change was preserved at all three tested values. Threshold-specific results are summarized in Table 8 and illustrated together with the inventory results in Figure 4.

At a threshold of 0.00, mapped area increased from 3.502 km² before the monsoon to 14.781 km² after the monsoon, producing a net increase of 11.280 km² and a post/pre factor of 4.22.

At the adopted threshold of 0.10, mapped area increased from 2.802 to 13.053 km², with a net increase of 10.250 km² and a post/pre factor of 4.66. At the more restrictive threshold of 0.20, mapped area increased from 1.995 to 11.516 km², with a net increase of 9.522 km² and a post/pre factor of 5.77.

Absolute areas decreased as the threshold became more restrictive. Nevertheless, a substantial post-monsoon increase was retained in every test, indicating that the directional result was robust although the mapped magnitudes were threshold-dependent.

4.7.2 Cleaned post-monsoon water-feature inventory

Following application of the five-pixel minimum-mapping filter, 532 post-monsoon water features were retained with a combined area of 1,259.876 ha (12.599 km²). Approximately 96.5% of the unfiltered post-monsoon area was retained. The size-class distribution is summarized in Table 9 and displayed in Figure 4.

Small features (<1 ha) were numerically dominant, with 333 features representing 62.6% of the count. Their combined area was 150.924 ha, equivalent to 12.0% of the inventory area.

Medium features (1–10 ha) numbered 175 and represented 32.9% of the count. A combined area of 521.603 ha, or 41.4% of the inventory area, was contributed by this class.

Only 24 large features (at least 10 ha) were identified, representing 4.5% of the count. However, 587.349 ha, or 46.6% of total inventory area, was contributed by this class. The largest mapped feature covered 88.909 ha.

A contrast was therefore observed between numerical abundance and areal contribution. Small features dominated the count, whereas almost half of the inventory area was contained in the limited number of large features. Hydrological function, storage capacity, ownership and engineering suitability could not be determined from mapped area alone.

Table 8. Sensitivity of pre- and post-monsoon surface-water area to MNDWI threshold.

MNDWI threshold	Pre-monsoon area (km²)	Post-monsoon area (km²)	Net increase (km²)	Post/pre factor
0.00	3.502	14.781	11.280	4.22
0.10	2.802	13.053	10.250	4.66
0.20	1.995	11.516	9.522	5.77

Table 9. Size distribution of the cleaned post-monsoon water-feature inventory.

Size class	Count	Count (%)	Area (ha)	Area (%)
Small, <1 ha	333	62.6	150.924	12.0
Medium, 1–10 ha	175	32.9	521.603	41.4
Large, at least 10 ha	24	4.5	587.349	46.6
Total	532	100	1,259.876	100

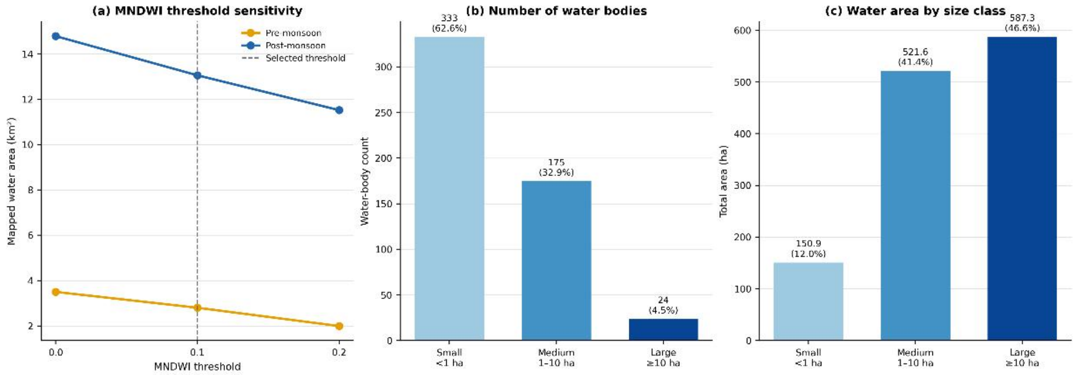

Figure 4. Sensitivity of mapped pre- and post-monsoon water extent to alternative MNDWI thresholds and size-class distribution of the cleaned post-monsoon water-feature inventory.

4.8 Sati outlet-sensitivity experiment

Methodological evidence of watershed sensitivity to outlet placement was provided by the attempted Sati delineation. Sati Nadi was identified from its name and approximate OSM alignment, but the mapped river line was found to be locally displaced from the terrain-controlled DEM channel.

Provisional and snapped outlet positions were tested near the expected downstream reach. Repeated attempts produced implausibly small upstream catchments that did not include the expected contributing drainage. These outputs were therefore rejected and were not reported as valid Sati watershed boundaries.

Proximity to a reference river line was shown to be insufficient for outlet validation. An outlet was also required to coincide with an appropriate flow-accumulation cell, to lie on the intended DEM-derived tributary and to maintain downstream connectivity with the receiving channel.

No basin area, perimeter, drainage density or other morphometric value was reported for Sati. The rejected outputs were retained only as evidence that hydrological connectivity must be verified before a watershed boundary is accepted.

4.9 Evidence synthesis across the five river systems

Different evidence levels were produced for the five regional river systems. Khobragadi was completed as the validated quantitative pilot and was represented by an accepted boundary, verified outlet, morphometric measurements, Strahler-order analysis and surface-water assessment.

Exploratory methodological evidence was produced for Sati rather than a completed basin analysis. Its provisional catchments were rejected because positional disagreement between the OSM line and DEM-derived channel resulted in hydrologically implausible delineations.

Bandia, Kathani and Gadhavi were documented at the regional-reference level. Named-river location, approximate alignment and broader drainage context were established, but validated outlets and boundaries were not available for basin-specific measurement.

The Khobragadi workflow can be transferred to the remaining systems only after each river alignment, confluence, flow-accumulation pathway, snapped outlet and resulting boundary have been independently verified.

The study should therefore be interpreted as one validated quantitative pilot, one exploratory outlet-sensitivity experiment and three regional-reference cases, rather than as a completed numerical comparison of five watersheds.

5. DISCUSSION

A multiscale analytical design was required because regional drainage characterization and basin-specific morphometry address different spatial and hydrological questions. HydroBASINS, MERIT Hydro and OpenStreetMap were effective for situating the Bandia, Khobragadi, Kathani, Sati and Gadhavi river systems within the broader Wainganga–Indravati drainage environment. The value of globally consistent hydrographic products for representing nested basin structure and regional river connectivity has been demonstrated previously (Lehner & Grill, 2013; Yamazaki et al., 2019). However, such products were not considered sufficiently precise for direct calculation of local watershed morphometry because differences in scale, generalization and positional accuracy can affect river alignment and outlet placement. Similar limitations have been reported for volunteered waterway data, for which spatial and temporal completeness may vary substantially (Monteiro & Patrício, 2024). Quantitative analysis was therefore restricted to the Khobragadi watershed because its outlet position and drainage connectivity satisfied the adopted validation criteria. This distinction prevented regional reference information from being interpreted as equivalent to a hydrologically validated basin boundary.

Drainage representation was influenced by both the 30 m NASADEM resolution and the selected flow-accumulation threshold. Narrow channels, small headwaters and locally modified pathways may have been generalized or omitted where their dimensions were below the raster resolution. At the lower thresholds of 1,000 and 2,500 cells, comparatively dense networks were produced, including numerous short segments that may have represented minor terrain convergence rather than persistent channels. In contrast, the 10,000-cell threshold omitted several intermediate tributaries and emphasized only the principal drainage pathways. The 5,000-cell threshold was therefore retained as a study-specific compromise between excessive drainage density and overgeneralization. Similar sensitivity of drainage-network properties to DEM resolution and extraction rules has been emphasized in global hydrographic and morphometric studies (Amatulli et al., 2022; Shekar & Mathew, 2024). Accordingly, the selected threshold should not be interpreted as universally optimal, because alternative thresholds would produce different total stream lengths, drainage densities, headwater distributions and maximum stream orders.

Lower-order channels dominated the validated Khobragadi network. Approximately 49.0% of the total extracted stream length was represented by first-order segments, whereas fifth-order channels contributed only 2.2%. This distribution indicates that the mapped drainage structure was primarily composed of numerous smaller tributary pathways connected to a limited higher-order network. Fifth-order organization was reached under the adopted extraction procedure. The calculated drainage density of 0.409 km km^{-2} should be interpreted specifically as the density of the network derived from the 30 m DEM using the 5,000-cell threshold. Morphometric studies conducted in Maharashtra have similarly shown that drainage characteristics can provide useful watershed information when the effects of DEM quality, extraction procedure and basin setting are recognized (Pande et al., 2021). However, drainage density alone cannot be used to infer high infiltration, groundwater recharge or subsurface permeability. Such interpretations would require independent information on geology, soils, land cover, rainfall and field hydrology.

Strong seasonal control over mapped surface-water availability was indicated by both the historical JRC analysis and the 2025 Sentinel-2 comparison. In the JRC dataset, 95.6% of historically detected water was classified as non-permanent or seasonal, while only 4.4% was classified as permanent. These results are consistent with the purpose of the JRC Global Surface Water product, which was developed to characterize long-term changes and persistence in mapped surface-water occurrence from Landsat observations (Pekel et al., 2016). The historical JRC result was kept analytically separate from the 2025 Sentinel-2 comparison because the datasets represent different observation periods, resolutions and classification definitions. In 2025, post-monsoon surface-water extent was 4.66 times the pre-monsoon extent. Most pre-monsoon water persisted, while most post-monsoon water was represented by seasonal expansion. The true-colour composites also showed more extensive visible water and darker vegetation after the monsoon. These findings indicate that monitoring should include both dry-season persistence and post-monsoon expansion rather than relying on a single seasonal observation. The broader value of multitemporal geospatial monitoring for agricultural water management has also been emphasized by Tarate et al. (2024).

A marked contrast was observed between water-body abundance and areal contribution. Features smaller than 1 ha represented 62.6% of the inventory count but only 12.0% of the total mapped area. In comparison, 24 large features contributed 46.6% of the inventory area. Small and medium features may be locally important because they increase the spatial distribution of surface water across the watershed. Nevertheless, hydrological function cannot be assigned from mapped area alone. Connectivity, depth, hydroperiod, ownership, water quality and structural condition were not evaluated. The inventory should therefore be treated as a screening baseline rather than as a direct basis for recommending ponds, check dams or recharge structures.

The direction of seasonal change was preserved at MNDWI thresholds of 0.00, 0.10 and 0.20. This consistency indicates that the principal conclusion of post-monsoon expansion was robust, although the absolute mapped areas remained threshold-dependent. The classification approach was based on the MNDWI method introduced by Xu (2006), but uncertainty remained because open-water indices can be affected by wet soil, terrain shadows, vegetation, turbidity and mixed pixels. Approximately 3.5% of the unfiltered post-monsoon water area was removed by the five-pixel minimum-mapping filter. This reduced isolated patches but may also have excluded genuine very small water features. Additional differences were introduced by the 30 m JRC resolution and the finer Sentinel-2 observations. Such sensor, threshold and class-definition effects are widely recognized in remote-sensing-based wetland and surface-water mapping (Yuan et al., 2025). Visual interpretation and field validation are therefore still required.

The Sati experiment demonstrated that outlet placement was a major source of watershed uncertainty. The OSM river line was locally displaced from the DEM-derived drainage pathway, and snapping based on proximity alone produced catchments that did not satisfy the validation criteria. Outlet validation was therefore required to consider flow accumulation, tributary identity and downstream connectivity. Methodological reliability was strengthened because only delineations that met the validation criteria were retained for quantitative interpretation. Before the Khobragadi procedure is transferred to Bandia, Kathani and Gadhavi, each river alignment, confluence, outlet position and resulting boundary must be independently verified.

The current evidence supports quantitative interpretation for Khobragadi only. Sati remains an exploratory outlet-sensitivity case, while Bandia, Kathani and Gadhavi remain regional-reference systems. Groundwater recharge, groundwater quality, pollution mitigation and conservation-structure suitability were not measured and cannot be inferred from the reported results. The Sentinel-2 seasonal assessment was limited to 2025, the JRC record ended in 2021 and basin-wide field verification was unavailable. Broader regional comparison will therefore require validated outlets, additional morphometric analysis, multiyear surface-water observations and independent hydrogeological and field measurements.

6. CONCLUSION

A multiscale GIS framework was established for regional drainage characterization and validated pilot-watershed assessment in Gondia and Gadchiroli districts. The five named river systems were placed within the broader Wainganga-Indravati drainage environment through regional hydrographic datasets, while reliable basin morphometry was shown to require a locally verified outlet and a hydrologically connected DEM-derived network. Alternative thresholds were tested with a conditioned 30 m NASADEM, and a 5,000-cell threshold was retained as a study-specific compromise because major and intermediate channels were preserved while excessive short segments were reduced.

The Khobragadi watershed was validated as the quantitative pilot. An area of 1,833.608 km^2, a perimeter of 408.676 km, 749.814 km of mapped streams and a drainage density of 0.409 km km^{-2} were obtained. Fifth-order organization was reached, and 49.0% of mapped stream length was represented by first-order segments. Historically detected surface water was dominated by the non-permanent or seasonal JRC class, and a 4.66-fold post-monsoon expansion was identified from the 2025 Sentinel-2 comparison. The direction of this seasonal increase was retained under all tested

MNDWI thresholds.

Outlet sensitivity and positional disagreement between reference lines and DEM-derived channels were demonstrated by the rejected Sati delineations. Uncertain catchments were therefore prevented from being reported as valid basin results. The findings represent one validated pilot, one exploratory outlet-sensitivity case and three regional-reference systems rather than a completed five-watershed comparison. Further regional analysis will require validated outlets, additional morphometry, multiyear water observations and field-based verification.

REFERENCES

1. Amatulli, G., Garcia Marquez, J., Sethi, T., Kiesel, J., Grigoropoulou, A., Üblacker, M., … Domisch, S. (2022). Hydrography90m: A new high-resolution global hydrographic dataset. Earth System Science Data, 14, 4525–4550. https://doi.org/10.5194/essd-14-4525-2022
2. Drusch, M., Del Bello, U., Carlier, S., Colin, O., Fernandez, V., Gascon, F., Hoersch, B., Isola, C., Laberinti, P., Martimort, P., Meygret, A., Spoto, F., Sy, O., Marchese, F., & Bargellini, P. (2012). Sentinel-2: ESA's optical high-resolution mission for GMES operational services. Remote Sensing of Environment, 120, 25–36. https://doi.org/10.1016/j.rse.2011.11.026
3. Geofabrik GmbH. (2026). OpenStreetMap data extract for Western Zone, India [GeoPackage dataset]. Geofabrik Download Server. https://download.geofabrik.de/asia/india/western-zone.html
4. Gorelick, N., Hancher, M., Dixon, M., Ilyushchenko, S., Thau, D., & Moore, R. (2017). Google Earth Engine: Planetary-scale geospatial analysis for everyone. Remote Sensing of Environment, 202, 18–27. https://doi.org/10.1016/j.rse.2017.06.031
5. Gunwant G. Wadpalliwar., Sapana P. Titirmare., Riya K. Kapkar and Samir B. Deshmukh. (2024). Morphometric Analysis of Gadhvi River, Sub-Basin Using Remote Sensing and GIS techniques. Gondwana Geological Society, Geosciences and Sustainable Development in Trible Areas, Vol. 3, 81-91. https://www.researchgate.net/publication
6. Gunwant G. Wadpalliwar., Samir B. Deshmukh. Raju G. Munghate. And Abhijeet P. Dharashiwkar (2024). Application of morphometric Study For Groundwater Management In Dongargarh Granite Around Kurkheda, District Gadchiroli, Maharashtra. International Research Journal of Management Science & Technology. Vol 15 Issue 3, 30-42. ISSN 2250 – 1959 (Online) 2348 – 9367 (Print) http://www.irjmst.com
7. Hou, Z., Zheng, D., Xiang, F., Bai, J., Chen, A., Ma, C., & Hou, M. (2025). Application of HydroSHEDS dataset in climate change and biodiversity evolution. Geological Journal of China Universities, 31(2), 238. https://doi.org/10.16108/j.issn1006-7493.2024023
8. Jagadeesha, C. J., & Manavalan, P. (2025). Advancing the use of geoinformatics-based water management. In Remote Sensing, GIS and Modelling for Water Resource Management: Volume 2 (pp. 509–535). Springer Nature Switzerland.
9. Lehner, B., & Grill, G. (2013). Global river hydrography and network routing: Baseline data and new approaches to study the world's large river systems. Hydrological Processes, 27(15), 2171–2186. https://doi.org/10.1002/hyp.9740
10. Lin, P., Pan, M., Wood, E. F., Yamazaki, D., & Allen, G. H. (2021). A new vector-based global river network dataset accounting for variable drainage density. Scientific Data, 8, 28. https://doi.org/10.1038/s41597-021-00819-9
11. Lindsay, J. B. (2016). Whitebox GAT: A case study in geomorphometric analysis. Computers & Geosciences, 95, 75–84. https://doi.org/10.1016/j.cageo.2016.07.003
12. Liu, Y., Wang, J., Liu, C., Huang, Y., Liu, Y., Liu, J., … Qu, W. (2026). An improved global river vector dataset based on multi-source river data fusion. Scientific Data, 13, 88. https://doi.org/10.1038/s41597-025-06399-2
13. Monteiro, E. S. V., & Patrício, G. R. (2024). Analysing temporal evolution of OpenStreetMap waterways completeness in a mountain region of Portugal. Remote Sensing, 16(17), 3159. https://doi.org/10.3390/rs16173159
14. NASA Jet Propulsion Laboratory. (2020). NASADEM merged DEM global 1 arc second V001 [Data set]. NASA EOSDIS Land Processes Distributed Active Archive Center. https://doi.org/10.5067/MEASURES/NASADEM/NASADEM_HGT.001
15. O'Callaghan, J. F., & Mark, D. M. (1984). The extraction of drainage networks from digital elevation data. Computer Vision, Graphics, and Image Processing, 28(3), 323–344. https://doi.org/10.1016/S0734-189X(84)80011-0
16. Pande, C. B., Moharir, K. N., & Khadri, S. F. R. (2021). Watershed planning and development based on morphometric analysis and remote sensing and GIS techniques: A case study of a semi-arid watershed in Maharashtra, India. In C. B. Pande and K. N. Moharir (Eds.), Groundwater Resources Development and Planning in the Semi-Arid Region (pp. 199–220). Springer. https://doi.org/10.1007/978-3-030-68124-1_11
17. Pekel, J.-F., Cottam, A., Gorelick, N., & Belward, A. S. (2016). High-resolution mapping of global surface water and its long-term changes. Nature, 540, 418–422. https://doi.org/10.1038/nature20584
18. Pierson, M., & Mehrabi, Z. (2024). Mapping waterways worldwide with deep learning. arXiv. https://doi.org/10.48550/arXiv.2412.00050
19. Shekar, P. R., & Mathew, A. (2024). Morphometric analysis of watersheds: A comprehensive review of data sources, quality, and geospatial techniques. Watershed Ecology and the Environment, 6, 13–25. https://doi.org/10.1016/j.wsee.2023.12.001
20. Singh, M. C., Satpute, S., & Prasad, V. (2023). Remote sensing and GIS-based watershed prioritization for land and water conservation planning and management. Water Science & Technology, 88(1), 233–265. https://doi.org/10.2166/wst.2023.207
21. Strahler, A. N. (1957). Quantitative analysis of watershed geomorphology. Transactions, American Geophysical Union, 38(6), 913–920. https://doi.org/10.1029/TR038i006p00913

22. Tarate, S. B., Patel, N. R., Danodia, A., Pokhariyal, S., & Parida, B. R. (2024). Geospatial technology for sustainable agricultural water management in India—A systematic review. Geomatics, 4(2), 91–123. https://doi.org/10.3390/geomatics4020006
23. Xu, H. (2006). Modification of normalised difference water index to enhance open-water features in remotely sensed imagery. International Journal of Remote Sensing, 27(14), 3025–3033. https://doi.org/10.1080/01431160600589179
24. Yamazaki, D., Ikeshima, D., Sosa, J., Bates, P. D., Allen, G. H., & Pavelsky, T. M. (2019). MERIT Hydro: A high-resolution global hydrography map based on latest topography dataset. Water Resources Research, 55(6), 5053–5073. https://doi.org/10.1029/2019WR024873
25. Yuan, S., Liang, X., Lin, T., Chen, S., Liu, R., Wang, J., … Gong, P. (2025). A comprehensive review of remote sensing in wetland classification and mapping. arXiv. https://doi.org/10.48550/arXiv.2504.10842